Journal of Structural Geology 31 (2009) 1028–1038

Contents lists available at ScienceDirect

Journal of Structural Geology

journal homepage: www.elsevier.com/locate/jsg

# Comparison of Fry strain ellipse and AMS ellipsoid trends to tectonic fabric trends in very low-strain sandstone of the Appalachian fold–thrust belt

K.C. Burmeister [a,*], M.J. Harrison [b], S. Marshak [c], E.C. Ferré [d], R.A. Bannister [c], K.P. Kodama [e]

[a] Dept. of Geosciences, University of the Pacific, 3601 Pacific Avenue, Stockton, CA 95211, USA
[b] Dept. of Earth Sciences, Tennessee Technological Univ., Box 5062, Cookeville, TN 38505, USA
[c] Dept. of Geology, Univ. of Illinois, 1301 W Green Street, Urbana, IL 61801, USA
[d] Dept. of Geology, Southern Illinois University, Carbondale, IL 62901-4324, USA
[e] Dept. of Earth & Environmental Sciences, Lehigh University, 31 Williams Drive, Bethlehem, PA 18015, USA

ARTICLE INFO

*Article history:*
Received 2 May 2007
Received in revised form
14 August 2008
Accepted 12 March 2009
Available online 24 March 2009

*Keywords:*
Tectonic fabrics
Anisotropy of magnetic susceptibility
AMS
Fry strain analysis
Appalachian fold–thrust belt
Hudson Valley fold–thrust belt
Rosendale
Lackawanna synclinorium

ABSTRACT

In moderately to highly strained sandstones, both the long axis of the bedding-parallel finite-strain ellipse, as calculated by the normalized Fry method, and the projection of the long axis of the AMS ellipsoid on the plane of bedding, align well with local "structural grain" (trends of cleavage, folds, and faults). This relationship implies that results of both 2D Fry and AMS analyses represent the local layer-parallel tectonic strain component. Do both methods provide comparable results for very *low-strain* sandstone (e.g., <5%)? To address this question, Fry and AMS analyses were conducted in very low-strain sandstone from two localities in the Appalachian foreland fold–thrust belt: near Rosendale in New York and the Lackawanna synclinorium of Pennsylvania. We compared the map projections of both bedding-parallel Fry ellipses and AMS ellipsoids to the local structural grain. In both study areas, projections of the long axis of Fry strain ellipses do not cluster in a direction parallel to structural grain, whereas the projection of the long axes of AMS ellipsoids do cluster closely to structural grain. This observation implies that in very low-strain sandstone, AMS analysis provides a more sensitive "quick" indicator of tectonic fabric than does normalized Fry analysis.



## 1. Introduction

In addition to the development of regional-scale thrust faults and related folds, tectonic shortening in foreland fold–thrust belts generates mesoscopic faults and folds, pressure-solution cleavage, and grain-scale deformation. At the low temperatures (<300 °C) under which foreland fold–thrust belts develop, grain-scale deformation yields pressure-solution pitting, twinning in calcite grains, and deformation bands in quartz grains. Cleavage and grain-scale deformation typically develop early during the deformation history and thus contribute to the accumulation of layer-parallel shortening (i.e., shortening in the plane of bedding). Layer-parallel shortening fabrics may develop far to the foreland of high-amplitude folding (e.g., Engelder, 1979).

In order to quantify layer-parallel shortening and define spatial variations in deformation kinematics within thrust sheets, several techniques for strain and rock-fabric analysis have been used for characterization of grain-scale deformation associated with layer-parallel tectonic strain. Studies focusing on clastic rocks commonly utilize either the 2D normalized Fry method of strain analysis to characterize strain in the plane of bedding (Fry, 1979; Erslev, 1988), or the study of anisotropy of magnetic susceptibility (AMS), for both methods yield results quickly. In rocks with strains greater than about 15%, Fry and AMS analyses clearly resolve tectonic shortening directions, because the map projection of the long axis of the bedding-plane 2D Fry strain ellipse, and the map projection of the long axis of the AMS ellipsoid, are parallel to structural grain defined by the map traces of folds, faults, and cleavage. In this paper, we address the question of whether the quick approach of using 2D Fry technique and the AMS technique can provide a reliable indicator of tectonic shortening in rocks with *very low strain*, here taken as strain of less than about 5%.

To address the above question, we compared strain-axis trends from both 2D bedding-plane Fry analysis and 3D AMS analysis to structural grain (trends of cleavage, folds, and faults). Our study utilizes reconnaissance data from two geographic regions in the foreland edge of the Appalachian fold–thrust belt: (1) the Rosendale region of the Hudson Valley fold–thrust belt in southeastern

* Corresponding author. Tel.: +1 209 946 2398; fax: +1 209 946 2362.
*E-mail address:* kburmeister@pacific.edu (K.C. Burmeister).

0191-8141/$ – see front matter © 2009 Elsevier Ltd. All rights reserved.
doi:10.1016/j.jsg.2009.03.010

New York (Burmeister, 2005); and (2) the Lackawanna region of the Valley and Ridge of northeastern Pennsylvania (Harrison, 2006). We found that the trend of the finite-strain long axes obtained using the 2D bedding-plane Fry method vary significantly relative to the structural grain in both study areas. In contrast, the map trend of the AMS-long axes in both study areas closely parallel structural grain. These results imply that AMS is a better "quick" indicator of tectonic fabric and, therefore, deformation kinematics, in very low-strain clastic sedimentary rock. Below, after briefly introducing the regional context of the two study areas, we provide the details of our methods and of our results. We conclude by speculating on the reasons for the differences between our Fry and AMS results.

## 2. Geologic setting of study areas

The Appalachian foreland fold–thrust belt encompasses the zone of thin-skinned, west- to northwest-verging deformation that developed along the eastern margin of North America in response to Paleozoic collisional orogenies. Along-strike changes in structural grain within this zone define distinct salients and recesses (e.g., Marshak, 2004, and references therein). Our project encompass two study areas within the fold–thrust belt: (1) the Rosendale region at the southern end of the Hudson Valley fold–thrust belt, in the core of the New York recess; and (2) the Lackawanna region, which includes the Lackawanna synclinorium, a structure that spans the boundary between the New York recess and the Pennsylvania salient (Fig. 1).

Though the two study areas occupy similar structural settings, they differ in that the fold–thrust belt of the Rosendale region is <8 km wide, measured perpendicular to strike, and first-order folds have wavelengths of less than 300 m, whereas the Lackawanna region extends into the Pennsylvania salient, where the fold–thrust belt attains a width of 140 km and first-order folds have wavelengths of up to 10 km. The dimensional contrast between these areas reflects the respective thickness of the deformed stratigraphic sequence of the two areas, for the width of fold–thrust belts is a function of the thickness of strata above the detachment (e.g., Marshak and Wilkerson, 1992).

### 2.1. Rosendale region

The Rosendale region lies south of Kingston, New York, at the southern end of the NNE-trending Hudson Valley fold–thrust belt (Fig. 1; Marshak, 1986; Burmeister, 2005). Deformation of the region involves a relatively thin sequence of Middle Ordovician through Middle Devonian strata (Fig. 2; Rickard, 1962; Waines and Hoar, 1967; Laporte, 1969), which can be divided into mechanically weak units, consisting primarily of shale, and mechanically rigid units, consisting either of sandstone or limestone.

Shortening above detachments within Ordovician strata produced several ramps that accommodated displacements of up to a few hundred meters and associated upright to inclined doubly plunging anticlines and synclines. Strata involved in the fold–thrust belt also contain a tectonic cleavage whose intensity and morphology vary locally as a function of initial clay content and local strain (e.g., Marshak and Engelder, 1985). Taken together, bedding strike, fault traces, fold-hinge traces, and cleavage traces of the Rosendale region define a distinct structural grain that trends 027° (Fig. 3). Because all strata involved in the Hudson Valley fold–thrust belt were deposited before both the Acadian and Alleghanian orogenies, the question of which event caused the observed deformation remains a subject of debate (Fisher, 1962; Rickard, 1962; Waines and Hoar, 1967; Rodgers, 1971; Waines, 1986; Marshak, 1986, 1990; Epstein and Lyttle, 1987; Marshak and Tabor, 1989).

### 2.2. Lackawanna region

The Lackawanna region encompasses the Lackawanna synclinorium, a 110 km-long by up to 15 km-wide structural trough, and adjacent areas in the Appalachian foreland of northeastern Pennsylvania (Fig. 1). The synclinorium involves Silurian through Pennsylvanian strata, but surface exposures provide access only to Devonian and younger units that include non-marine quartz-lithic

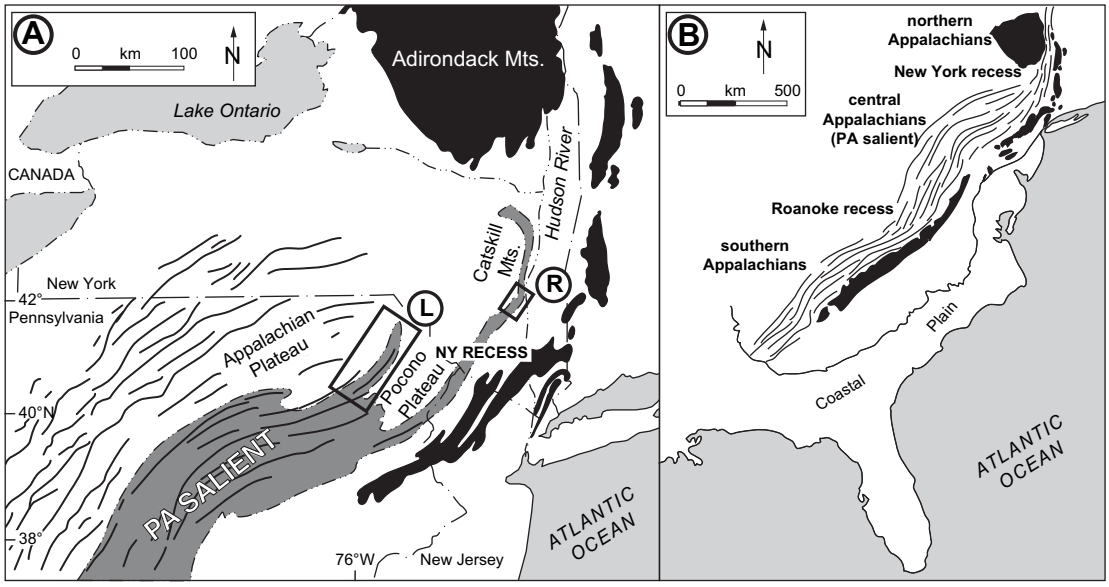


**Fig. 1.** (A) Regional location map showing the location of the Hudson Valley fold–thrust belt and the Valley and Ridge Province segments of Appalachian fold–thrust belt. (B) Simplified structure map of New York recess within the Appalachian orogen of eastern North America. Heavy lines indicate fold traces, dark gray areas delineate exposure of deformed Silurian and Devonian strata, and black areas delineate exposures of Precambrian crystalline basement. Boxes outline locations of study areas within the Rosendale (R) and Lackawanna (L) regions.

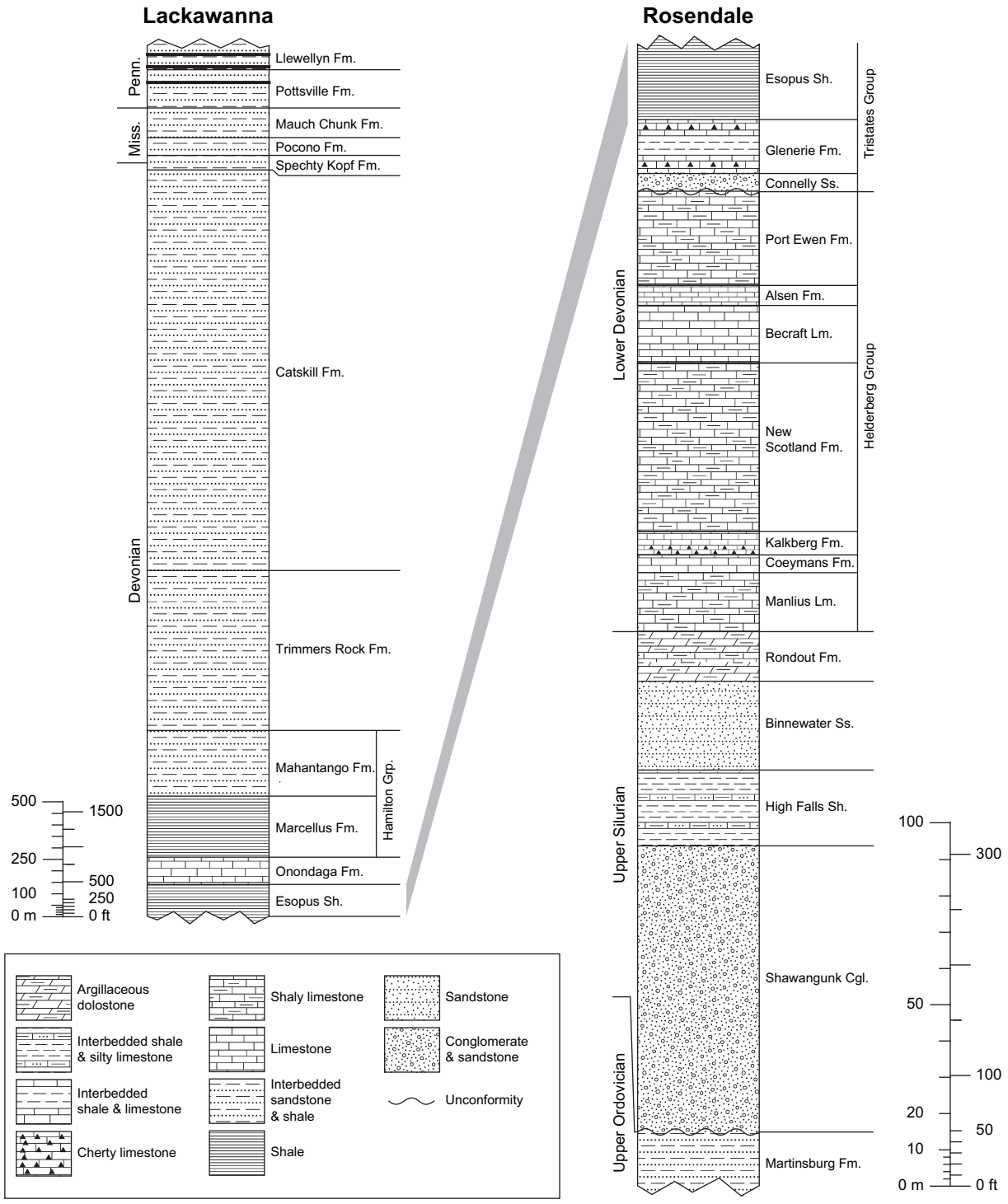


**Fig. 2.** Stratigraphy of the Rosendale (southeastern New York State) and Lackawanna (northeastern Pennsylvania) regions within the Appalachian foreland. For further description of the stratigraphy of the Rosendale region, see Waines and Hoar (1967), Marshak and Tabor (1989), and Burmeister (2005). For further description of the Lackawanna region stratigraphy, see Harrison (2002).

arenite with interbedded conglomerate, siltstone, shale, and coal (Fig. 2; Harrison et al., 2004).

The Lackawanna synclinorium originated as a north-trending salt-collapse feature, but it was tectonically modified by the Alleghanian orogeny so that its southern end became incorporated in thin-skinned thrusting and, as a consequence, was rotated clockwise in map view (Harrison et al., 2004; Harrison, 2006). The synclinorium, therefore, displays concave-to-the-foreland curvature. Specifically, its northern arm trends 010°, at a high angle to the trends of the Appalachian Plateau's very gentle folds, whereas its southern arm trends 075°, and lies within the northeastern arm of the Pennsylvania salient (Fig. 4). Topographically, therefore, the northern part of the synclinorium is an elongate depression, relative to the surrounding plateau, whereas the southern part lies within the Appalachian Valley and Ridge. Of note, numerous ENE-trending second-order folds involve Mississippian

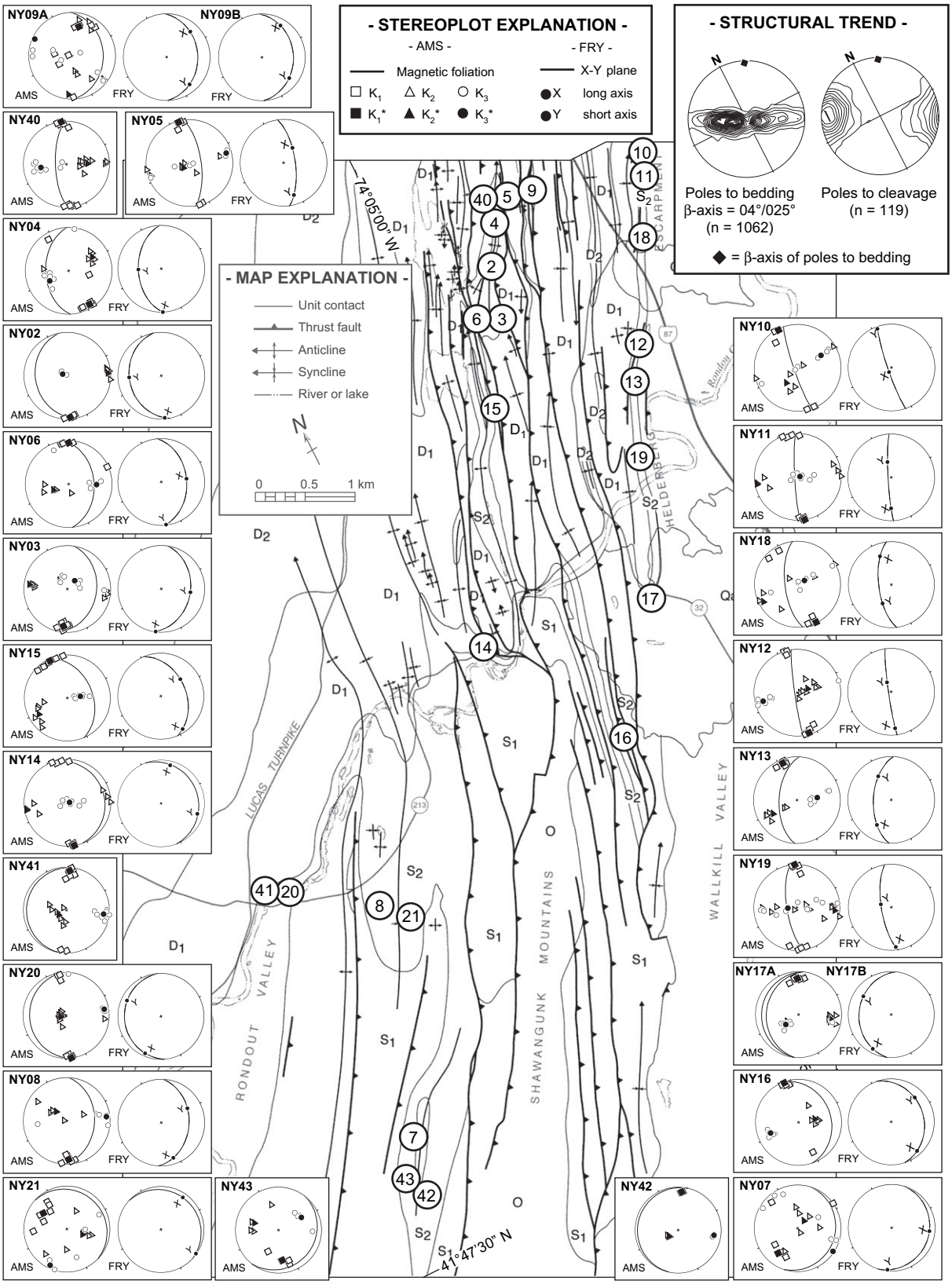


**Fig. 3.** Simplified geologic map of the Rosendale region showing sample locations within the Binnewater Formation. Geologic map units include: Martinsburg Shale (O); Shawangunk Conglomerate (S1); High Falls, Binnewater, and Rondout Formations (S2); Manlius, Coeymans, Kalkberg, New Scotland, Becraft, Alsen, Port Ewen, Connelly, and Glenerie Formations (D1); Esopus Shale (D2); Schoharie and Onondaga Formations (D3); and glacial deposits (Qa). The regional structural trend, illustrated by lower-hemisphere, equal area stereographic projections of poles to bedding and poles tectonic cleavage in Late Silurian through Middle Devonian strata, is provided for reference at upper right; the Kamb contour interval is 2.0 sigma, significance level is 3.0 sigma. Also shown are the lower-hemisphere projections of bedding and the AMS and Fry fabrics measured at each sample location. The $K_1$ axes and the magnetic foliation ($K_1$–$K_2$), as defined by AMS analysis, and the X axes within the flattening plane (X–Y), as defined by Fry analysis, are shown with bold lines. Note all stereoplots are rotated 27° counterclockwise to correspond to the map orientation.

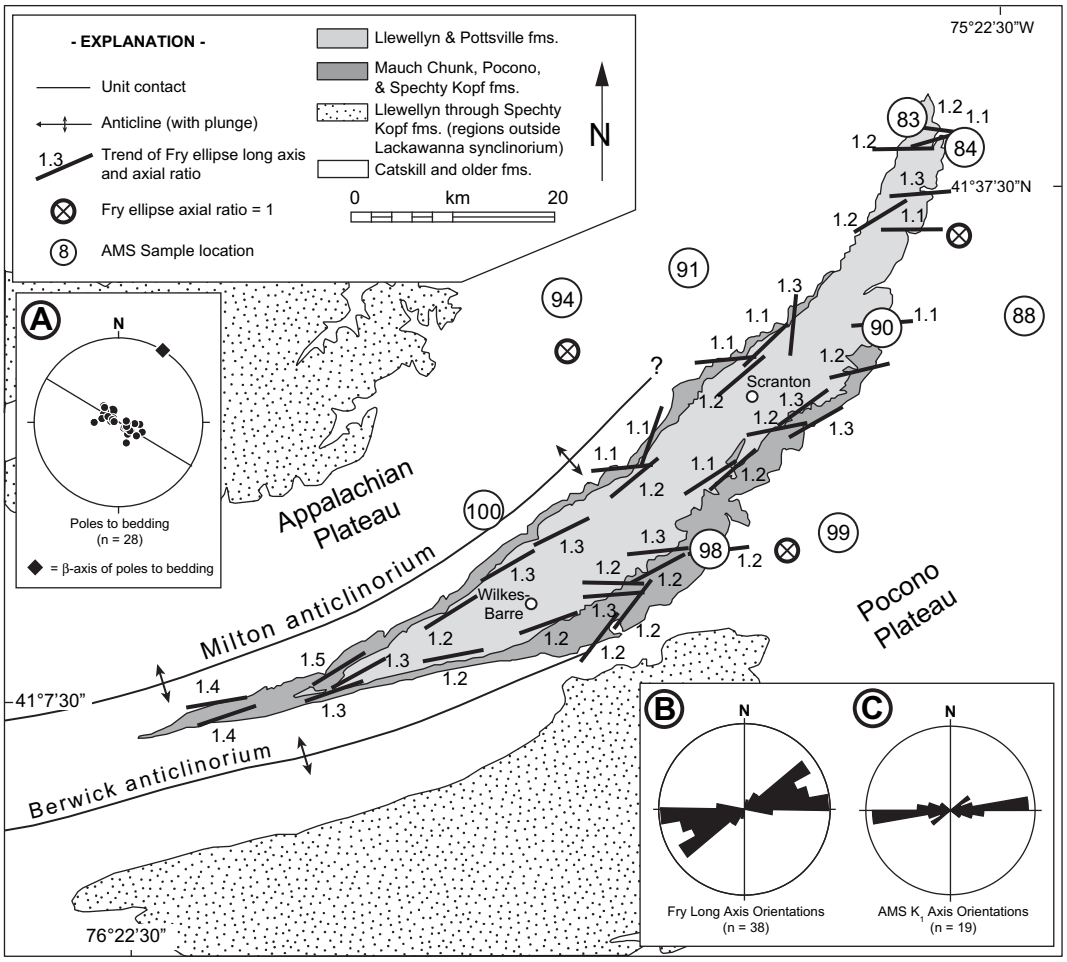


**Fig. 4.** A simplified geologic map of the Lackawanna region. (A) The lower-hemisphere stereoplot illustrates poles to bedding in the study area. Symbols illustrating long-axis trends and axial ratios of individual bedding-parallel Fry ellipses correspond with sampling locations throughout the study area. Rose diagrams summarize (B) the trends of the long axes of bedding-parallel Fry ellipses and (C) the trends of all the $K_1$ axes of AMS fabrics measured within the study area.

and Pennsylvanian strata above the regional Pottchunk detachment within the hinge zone of the Lackawanna Synclinorium. These folds trend parallel to the regional hinge of the Lackawanna synclinorium in the southern end of the structure, but trend nearly perpendicular to the regional hinge in its northern end (Harrison, 2006).

## 3. Sampling and analytical methods

In both study areas, we collected oriented samples for normalized Fry analysis and AMS analysis from outcrops that contained obvious tectonic structures (folds, faults, and cleavage). Care was taken to collect fresh rock with uniform composition, and to avoid strata containing complex bedforms, bioturbation, and other sedimentary structures that might impart primary fabrics. This study combines the results of two separate studies that used somewhat different sampling and analytical methods, but all methods used are standard.

### 3.1. Fry analysis procedures

The Fry method determines 2D finite strain by measuring center-to-center distances between anticlustered particles in a photomicrograph (Fry, 1979). Erslev (1988) modified the method by normalizing the center-to-center distances to reduce the influence of 2D grain size. The result produces a better-defined strain ellipse and is now called the "normalized Fry method" (Erslev, 1988; Dunne et al., 1990). 2D normalized Fry studies of bedding-plane strain in sandstone (i.e., mechanically strong beds) is assumed to be a proxy for layer-parallel tectonic shortening, for pre-deformation compaction tends to occur perpendicular to bedding.

Twenty-one samples of Binnewater Formation from the Rosendale region were analyzed for 2D bedding-parallel strain with the normalized Fry method (Burmeister, 2005). To obtain the images needed for the analyses, we prepared photomicrographs of oriented standard thin sections. The computer program *ELLIPSEFIT* (©1998 F.W. Vollmer) was used to locate at least five points along the boundaries of 250 grains in each digital photomicrograph. Cathodoluminescence analysis of the Binnewater Sandstone samples was conducted to detect optically continuous overgrowth cements that might obscure original grain boundaries and produce errors in calculating grain centers (see Dunne et al., 1990). *ELLIPSEFIT* calculated the best-fit ellipsoid for each grain; the center of this ellipsoid was taken as the grain center. *ELLIPSEFIT* also produced a normalized Fry plot using the calculated grain centers, calculated the best-fitting strain ellipse for the central void of the plot, and specified the X and Y axes of the strain ellipse. Finally, the program calculated axial ratio ($R_s$) and the rake ($\varphi$) of the X-axis, relative to strike. Digital images were managed within *ADOBE PHOTOSHOP* by using a Java script that normalized image scale and quality and embedded sample-orientation information (Bannister et al., 2004).

In the Lackawanna study area, 37 oriented samples of quartz arenite, predominately from the Pottsville and Llewellyn Formations, were analyzed for 2D bed-parallel strain using the normalized Fry method (Harrison, 2002). Grain centers were determined by visually digitizing the long and short axes of each framework grain. The computer program *INSTRAIN* (Erslev, 1988) calculated the center for each grain, by using the points defined by the ends of the long and short axes. 200–300 quartz grains were digitized on each photomicrograph. Cathodoluminescence analysis of the samples revealed trace amounts of quartz overgrowth cement, but a comparison of Fry strain ellipse orientations and strain ratios from cathodoluminescence and cross-polarized photomicrographs yielded only nominal differences, suggesting that the trace quantities of quartz overgrowth cement did not influence strain measurements. Thus, cross-polarized photomicrographs alone were used for the Fry analysis. Strain ellipses were drawn by hand on normalized Fry plots generated by *INSTRAIN*.

### 3.2. AMS analysis procedures

Magnetic susceptibility is the ratio between the inducing field and the induced magnetization of a material. Both field and magnetization are specified using the same units (Amperes/meter) therefore magnetic susceptibility is a dimensionless number. The magnetic susceptibility of a specimen generally varies with the direction of the inducing field. The resulting anisotropy of magnetic susceptibility (AMS) originates primarily from the following factors: (1) the shape preferred orientation (SPO) of ferromagnetic (*sensu lato*) minerals; (2) the lattice preferred orientation (LPO) of paramagnetic and diamagnetic minerals; and (3) the distribution anisotropy of ferromagnetic grains within a specimen (e.g., Hrouda, 1982; Rochette, 1987; Borradaile, 1988; Hargraves et al., 1991). The AMS can be approximated by second-rank tensor, and thus can be represented by an ellipsoid with three mutually perpendicular principal axes: maximum ($K_1$), intermediate ($K_2$), and minimum ($K_3$). The magnetic lineation is defined by $K_1$ while the magnetic foliation is defined by the plane containing $K_1$ and $K_2$.

The measurement of AMS can help characterize penetrative tectonic fabrics in weakly deformed rocks because AMS is sensitive to even slight preferred orientations of magnetic minerals (e.g., Fuller, 1964; Kligfield et al., 1977; Rathore, 1979; Borradaile and Tarling, 1981; Borradaile, 1991; Kissel et al., 1986; Lowrie and Hirt, 1987; Aubourg et al., 1991; Averbuch et al., 1992; Parés et al., 1999; Lüeneburg et al., 1999). However, while the correlation between the orientations of AMS principle axes and strain principle axes tends to be very consistent, correlations between the magnitudes of AMS axes and corresponding strain axes is not (e.g., Evans and Elmore, 2006; Latta and Anastasio, 2007).

For the AMS component of our study, we collected thirty-three oriented block samples in the field. 24 of these were in Binnewater Sandstone outcrops of the Rosendale area, and the remaining 9 were in Catskill and Spechty Kopf Formations of the Lackawanna area. Specimens were prepared in the lab from the block samples—from the Rosendale blocks we cut a total of 166 cubes that were 20 mm on a side, and from the Lackawanna blocks we cut a total of 55 cores that were 25.4 mm-diameter × 22 mm-length cores. An average of 5 cubes or cores were analyzed for each sample site.

The AMS of Rosendale specimens was measured in low-field (300 A/m, 920 Hz) on a magnetic susceptibility bridge (Kappabridge KLY-3S) at Southern Illinois University, and for the Lackawanna samples, we used similar equipment at Lehigh University; see Tarling and Hrouda (1993) and Jelinek et al. (1997) for a description of methodology. Instrument precision for AMS measurements was >99%. Determination of this instrumental error demonstrated that the principal directions are meaningful when $P_j > 1.003$. The hysteresis properties of the Binnewater Sandstone specimens from the Rosendale region were determined using a Princeton Measurements *MicroMag 3900-4* vibrating sample magnetometer at the University of Minnesota's Institute of Rock Magnetism. The natural remnant magnetization (NRM) of Lackawanna region samples was measured using a *Molspin Minispin* fluxgate spinner magnetometer at Lehigh University.

## 4. Observations and results

### 4.1. Petrography of samples

The Binnewater Sandstone of the Rosendale region consists of a texturally immature quartz wacke (Fig. 5; Wanless, 1921; Waines and Hoar, 1967; Waines, 1976; Burmeister, 2005). Clay- and silt-rich matrix forms <5% to 20% of rock volume, but locally accounts for as much as 80% of rock volume. Cathodoluminescence microscopy reveals minimal optically continuous overgrowth cement. Hematite cement or grain coatings were not observed in any hand samples or thin sections. The presence of local clay selvages between grains, and of quartz grains with truncated, sutured, and interpenetrated boundaries, indicates that the rock underwent pressure-solution deformation. Post-depositional brittle deformation produced local antitaxial fibrous quartz microveins, thin cataclastic bands, and microcracks in the unit.

The Catskill Formation of the Lackawanna region consists predominantly of quartz arenite, with ~5–10% matrix that contains clay, iron oxide grain coatings, and mica. Grain size in the Catskill Formation ranges from fine to medium sand. Samples of the Pottsville Formation used in this study consist of fine- to medium-grained quartz arenite, with <10% clay matrix and rock fragments. Some of the samples contain iron oxide coatings on grains, and macroscopically are reddish brown (i.e., are redbeds). However, others do not and macroscopically are light tan- to green-grey. Pressure solution resulted in the production of sutured and interpenetrating grains. Llewellyn Formation samples of the Lackawanna region contain up to 15% clay matrix and rock fragments, but otherwise are similar to those from the Pottsville Formation.

### 4.2. Fry and AMS results for the Rosendale region

2D normalized Fry analysis indicates that the Binnewater Sandstone of the Rosendale region accumulated only very small bedding-parallel shortening strains. Ellipse axial ratios range between 1.02 and 1.20, with a mean of 1.08 (Appendix 1). Binnewater Sandstone specimens region also display relatively low magnetic susceptibilities ($<110 \times 10^{-6}$ [SI]; Appendix 2). The hysteresis properties of the Binnewater Sandstone samples are characteristic of multi-domain magnetite grains that exceed 10 μm in length (Fig. 6A and Table 1; Butler, 1992), and the high-field slopes of the hysteresis curves indicate that their susceptibility has relatively large ferromagnetic and relatively small paramagnetic components.

Table 1 provides the results of AMS analysis for Rosendale region samples, and Fig. 3 illustrates the orientations of the $K_1$ axes. The bulk magnetic susceptibility ($K_m$, which is the arithmetic mean of the principal susceptibilities) generally falls between $-9 \times 10^{-7}$ [SI] and $120 \times 10^{-6}$ [SI] and has an average of $\approx 47 \times 10^{-6}$ [SI]. The corrected degree of anisotropy ($P_j$), and the AMS fabric-ellipsoid shape ($T_j$) at each sample location was calculated using the tensor-averaging method of Jelinek (1978). We found that total anisotropy ranges from 1.002 to 2.821, but is generally low with an average of 1.041. The AMS ellipsoids are only slightly non-spherical and range from highly prolate to highly oblate (Fig. 6B); the magnetic foliation

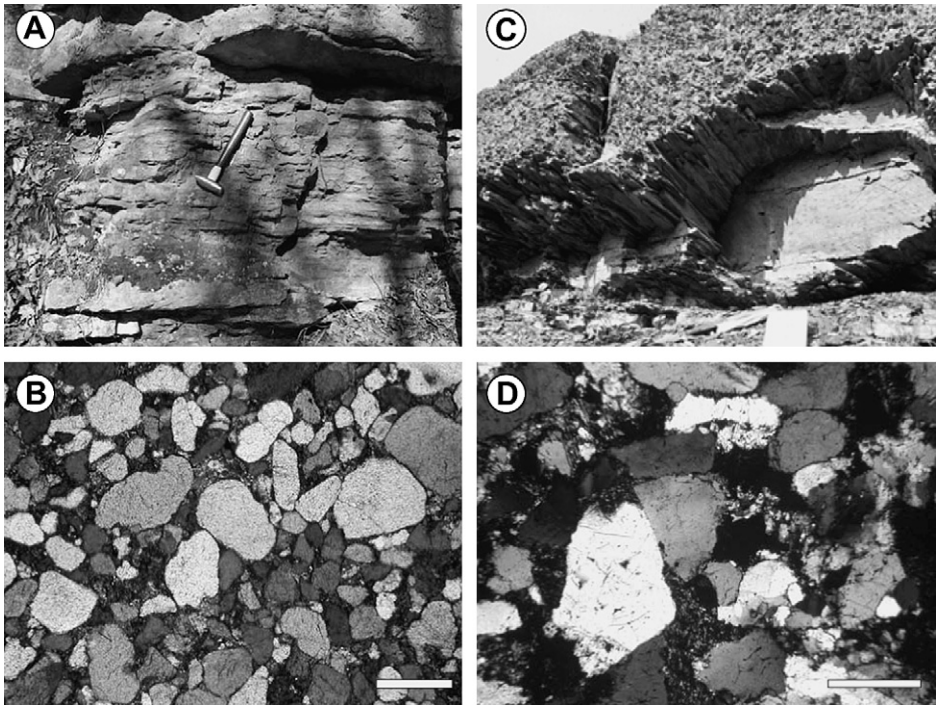


**Fig. 5.** (A) Photograph of the Binnewater Sandstone in outcrop; (B) photomicrograph of the Binnewater Sandstone. Arrows point to embayed and sutured grain margins from pressure solution (scale bar is 0.5 mm). (C) Outcrop photograph of cleavage (pencil structures) in siltstone of the Llewellyn Formation in the Lackawanna region. These structures are located in the core of a mesoscopic fold and the long dimensions of pencils are oriented 075°. (D) Representative photomicrograph of Llewellyn Formation sandstone under crossed-polarized light (scale bar is 0.5 mm). Large grains are quartz with clay matrix in bottom center and folded muscovite in upper left.

is commonly inclined at an angle to bedding. The shape magnetic susceptibility displays no correlation with either the degree of anisotropy (Fig. 6C) or with the shape of the magnetic fabric ellipsoid (Fig. 6D). The mean value for $T_j$ is −0.019.

### 4.3. Fry and AMS results for the Lackawanna area

For samples from the Lackawanna region, axial ratios of bedding-parallel strain ellipses, based on normalized Fry analysis, range from 1.1 to 1.3 (±0.1) and decrease progressively from south to north in the field area (Fig. 4; Appendix 1). This decrease corresponds to a progressive south to north decrease in the amplitude of second-order folds above the Pottchunk fault. The trend of the finite-strain long axes also varies from south to north along the length of the synclinorium. Specifically, in the southern synclinorium where the ellipticity of the strain ellipses is greater, the long axes of these strain ellipses trend between 060° and 070°, i.e., parallel to the outcrop-scale fabrics. However, in the central and northern synclinorium where the ellipticity of the strain ellipse is smaller, the orientation of the long axes is bimodal, with one set trending between 050° and 060° and another trending 080° and 090° (Fig. 4).

Bulk magnetic susceptibilities in Lackawanna region samples range from ~5 to $400 \times 10^{-6}$ [SI], with most samples over $200 \times 10^{-6}$ [SI]. Appendix 2 shows the magnitude of the bulk susceptibility, anisotropy factors $P_j$ and T, and the orientation of the susceptibility axes. Measurements of NRM indicate that the non-redbed sandstone samples (mostly light tan to dark green) have magnetic intensities ranging from 0.15 to $6.23 \times 10^{-3}$ A/m, whereas a representative redbed sandstone sample yielded an intensity of about $100 \times 10^{-3}$ A/m. These results, along with petrographic investigations, suggest that hematite is the dominant carriers of AMS in redbeds and that phyllosilicates are the dominant carriers in the non-redbed samples.

Fig. 4B shows the trend of the magnetic susceptibility axes for samples from the Lackawanna region. The mean trend of $K_1$ is 086°, with $K_1$ lying in the plane of bedding. In all samples except PA90 and PA98, $K_3$ is normal to bedding, $K_2$ is sub-parallel to the regional shortening direction, and $K_1$ is normal to the shortening direction (parallel to the regional LPS fabric). In sample PA98, $K_1$ is parallel to the regional shortening fabric, but $K_3$ and $K_2$ are dispersed about a great-circle girdle sub-parallel to the regional shortening direction. In sample PA90, $K_1$ is sub-parallel to the shortening direction and $K_2$ lies sub-parallel to the structural grain. In sample PA91, the $K_1$ orientation is at a moderate angle to the structural grain. Overall, the $K_1$ axes trend sub-parallel to the fold hinges on the plateau and to cleavage within the synclinorium.

## 5. Discussion

A study of the map projections of the long axis of the AMS ellipsoid, and of the bedding-parallel finite-strain ellipse calculated by the normalized Fry method, shows that in very low-strain rocks, the former is consistently closer to the trend of structural grain (defined by trends of faults, cleavage, and fold hinges) in a region (Figs. 3 and 5). Fig. 7, a synoptic plot showing trends of the $K_1$ axes calculated from AMS measurements, trends of long axes of strain calculated from Fry measurements, and trends of structural grain emphasizes this result. In the Rosendale region, the mean deviation of the Fry finite-strain long axes from the structural grain (027°) is ±35°, whereas the mean deviation of $K_1$ from the structural grain is ±17°. In the Lackawanna area, the mean deviation of the Fry finite-strain long axes from the structural grain (070°–082°) is ±15°, whereas the mean deviation of $K_1$ from the structural grain is ±8°. (Sample PA90 from the Lackawanna area does not fit the pattern. It

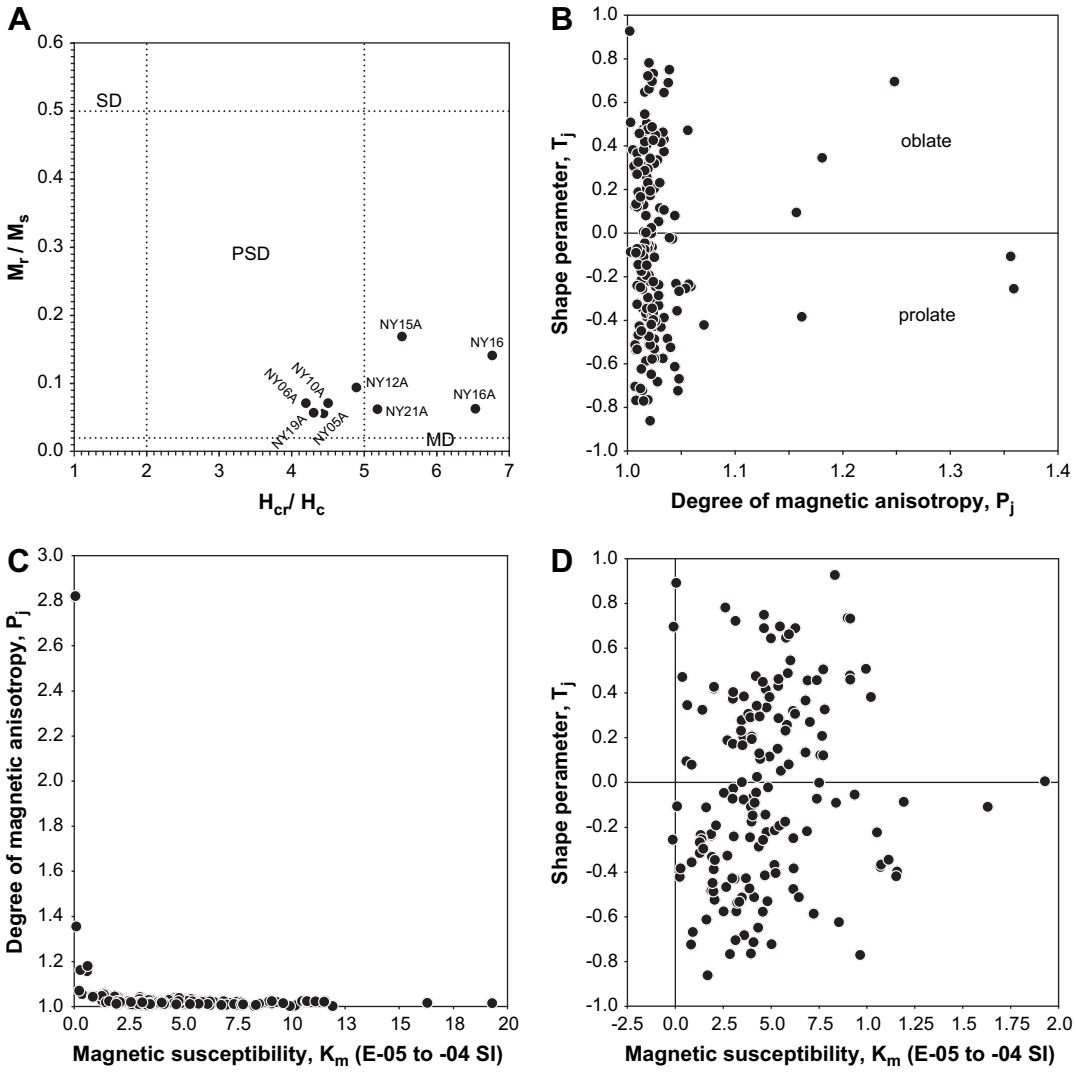


**Fig. 6.** (A) This graph provides a plot of the hysteresis parameters of samples collected from the Binnewater Sandstone (following the format of Day et al., 1977). (B) A plot of the shape parameter versus the degree of magnetic susceptibility in Binnewater Sandstone specimens. Note that magnetic fabric ellipsoids are only weakly eccentric and have a broad range of shapes. (C) A plot showing the degree of magnetic anisotropy; (D) A plot showing the shape parameter; note that it does not show any correlation with the magnetic susceptibility.

may have been affected by local fluid alteration, as suggested by iron oxide staining in underlying units.) Notably, the parallelism of the strain ellipse long axis and tectonic grain improves as strain increases, as illustrated by the north to south increase of strain ratios within the Lackawanna synclinorium (Fig. 4). Our results are compatible with previous studies that have also noted the parallelism of $K_1$ and the cleavage-bedding intersection in low-strain rocks (e.g., Kligfield et al., 1977; Rathore, 1979; Borradaile, 1991; Saint-Bezar et al., 2002; Parés and van der Pluijm, 2003).

Does the parallelism of AMS with strain reflect growth of new magnetic carriers during deformation, or is it due to reorientation of detrital grains during deformation? Our study indicates that the magnetic fabric in the Binnewater Sandstone of the Rosendale region comes from multi-domain grains of magnetite within the

**Table 1**
Results of hysteresis and resistivity analyses of representative samples of Binnewater Formation conducted at the Institute for Rock Magnetism, University of Minnesota.

| Specimen | $M_r$ ($\mu Am^2$) | $M_s$ ($\mu Am^2$) | $M_r/M_s$ | $H_c$ (mT) | $H_{cr}$ (mT) | $H_{cr}/H_c$ | $X_{HF}$ ($\mu Am^2/T$) |
|---|---|---|---|---|---|---|---|
| NY05A | 1 | 11 | 0 | 7 | 33 | 4 | +206 |
| NY06A | 1 | 10 | 0 | 10 | 42 | 4 | +25.3 |
| NY10A | 0 | 7 | 0 | 9 | 40 | 5 | +22.2 |
| NY12A | 1 | 8 | 0 | 7 | 34 | 5 | +82.2 |
| NY15A | 2 | 11 | 0 | 28 | 154 | 6 | +187 |
| NY16 | 1 | 6 | 0 | 12 | 78 | 7 | +203 |
| NY16A | 1 | 12 | 0 | 11 | 69 | 7 | +211 |
| NY19A | 0 | 7 | 0 | 7 | 29 | 4 | +268 |
| NY21A | 1 | 12 | 0 | 7 | 39 | 5 | 190 |

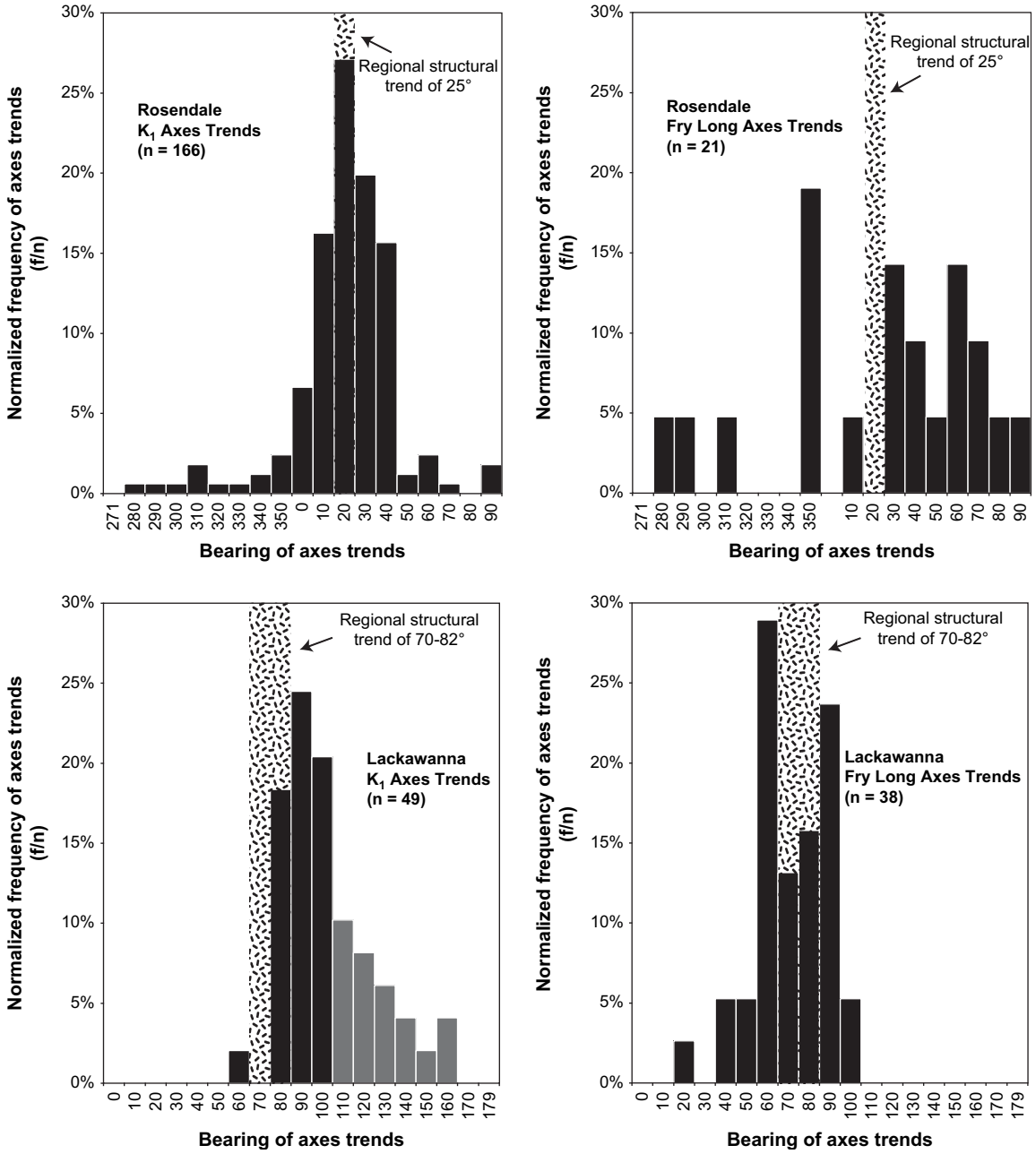


**Fig. 7.** Normalized histograms showing the trend of the long axes of bedding-parallel Fry ellipses and the $K_1$ axes of AMS ellipsoids relative to the regional structural trends in the Rosendale and Lackawanna regions. Normalized frequencies reflect the percentage of the data set containing a range of axes trends. Lackawanna $K_1$ azimuths of 122–155° correspond to sample PA90, which was likely affected by faulting and fluids. Also, Lackawanna $K_1$ azimuths of 114–128° correspond to sample PA91. Sample PA91 was collected from an outcrop that contains a cleavage-bedding intersection lineation that trends ~095°. Axis trends from samples PA90 and PA91 are illustrated with gray bars in the Lackawanna $K_1$ histogram.

matrix. These grains are large enough to be seen (if not obscured by matrix), and are roughly equant in size, suggesting that they have been hydrodynamically sorted and are not a consequence of diagenetic alteration of smectite, or of syndeformation growth. Thus, the AMS fabrics in the Binnewater Sandstone appear to reflect slight bulk rotation of detrital grains within the matrix during deformation and formation of the regional tectonic fabric.

We suggest that the discordance between the finite-strain axes calculated by the normalized Fry technique and the structural grain is due to the following factors:

(1) The basis for calculation using the Fry method has inherent inaccuracies at low strain because the original ellipticity of grains may be similar to or even exceed the imposed tectonic ellipticity. Thus, the determination of grain centers may not be accurate, regardless of whether the centers are determined visually or by computer programs such as *ELLIPSEFIT*. Thus, results simply might not represent the true tectonic strain.
(2) In very low-strain samples, an apparent linear trend detected by 2D Fry analysis may simply reflect the intersection of a planar fabric with the plane of the thin section, if the thin-section plane is not exactly parallel to bedding.
(3) The measured finite strain represents the sum of all strain increments that the rock has endured (e.g., Gray and Stamatakos, 1997; Gray and Mitra, 1999). Thus, the measured ellipsoid may be a composite of unrelated fabrics—primary

compactional strain (Onasch, 1994; Onasch et al., 1998), and tectonic strain. In fact, Paterson and Yu (1994) and Wetmore (2003) show that undeformed sandstone can contain significant 3D primary fabrics that are of equal magnitude to the tectonic strains measured using the Fry method. Notably, rocks with weak pre-deformational fabrics more accurately record tectonic deformation than so those that have a strong fabric (Parés and van der Pluijm, 2002), so spatial variability in the degree of compaction can lead to variability in the trend of strain ellipses measured by the Fry technique.

(4) Local (grain-scale to hand-specimen scale) rock heterogeneities may lead to local refraction of strain that cannot be detected by mesoscale visual observation. Similarly, viscosity contrasts between strain markers and matrix may cause strain markers to record less strain than the matrix (Treagus, 2002), and physical interactions among particles may lead to strain shadows or local grain rotation.

(5) Inhomogeneous changes to the volume of the markers, due to pressure solution, or to the volume of the matrix (e.g., due to dewatering of clays) may affect measured strain magnitudes independently of tectonic shortening directions (Ramsay and Wood, 1973; Dunne et al., 1990; Onasch and Dunne, 1993).

## 6. Conclusions

Analysis of samples from the Appalachian fold–thrust belt in the Rosendale (New York) and Lackawanna (Pennsylvania) regions indicate that, in very low-strain sandstones, the map projections of the long axis ($K_1$) of AMS ellipsoids provide a more accurate representation of tectonic structural grain than do map projections of bedding-plane 2D strain ellipsoids measured using the normalized Fry technique. Thus, AMS measurements are a better "quick" technique for detecting grain-scale tectonic strain in the foreland region of a fold–thrust belt, perhaps because they reflect grain reorientation of detrital carriers in the weaker matrix of rock and are more sensitive to subtle amounts of shortening. The inherent inaccuracy of the normalized Fry method in very low-strain rocks may be reflect the following: the measured finite-strain ellipsoid is a composite of primary (depositional or compactional) and tectonic fabrics; strain may be influenced by viscosity contrasts between markers and matrix, particle interactions; and strain may be affected by marker volume.

## Acknowledgements

This work was funded by the USGS EDMAP program, the Geological Society of America, Sigma Xi, and the Leighton Fund of the Department of Geology at the University of Illinois. The manuscript benefited greatly from thorough reviews by D. Anastasio and an anonymous reviewer, and thoughtful discussions with H. Alsleben, G. Pignotta, R.H. Waines, and P.H. Wetmore. The Century House Historical Society, D. Werner, and G. Grunwald generously provided logistical support of fieldwork at Rosendale. Thanks also to M. Jackson for coordinating the use of equipment at the Institute for Rock Magnetism at the University of Minnesota, and to F.A. Corsetti for the use of the cathodoluminesence lab at the University of Southern California. Finally, we gratefully acknowledge F.W. Vollmer and S.R. Paterson for the use of their respective computer programs.

## Appendix. Supplementary data

Supplementary data associated with this article can be found in the online version, at doi:10.1016/j.jsg.2009.03.010.

## References

Aubourg, C., Rochette, P., Vialon, P., 1991. Subtle stretching lineation revealed by magnetic fabric of Callovian–Oxfordian black shales (French Alps). Tectonophysics 185, 211–223.

Averbuch, O., Frizon, d.L.D., Kissel, C., 1992. Magnetic fabric as a structural indicator of the deformation path within a fold–thrust structure; a test case from the Corbieres (NE Pyrenees, France). Journal of Structural Geology 14, 461–474.

Bannister, R.A., Burmeister, K.C., Marshak, S., 2004. Using JavaScript to standardize digital photomicrographs for Fry strain analysis: Binnewater Sandstone, central Hudson Valley, New York. Abstracts with Programs. Geological Society of America 36, 41–42.

Borradaile, G.J., 1988. Magnetic susceptibility, petrofabrics and strain. Tectonophysics 156, 1–20.

Borradaile, G.J., 1991. Correlation of strain with anisotropy of magnetic susceptibility (AMS). Pure and Applied Geophysics 135, 15–29.

Borradaile, G.J., Tarling, D.H., 1981. The influence of deformation mechanisms on magnetic fabrics in weakly deformed rocks. Tectonophysics 77, 151–168.

Burmeister, K.C., 2005. Aspects of Deformation and Strain in the Appalachian Fold–Thrust Belt (New York) and the Shear Zones of the Sveconorwegian Orogen (Norway). Ph.D. thesis, University of Illinois.

Butler, R.F., 1992. Paleomagnetism; Magnetic Domains to Geologic Terranes. Blackwell Sci. Publ., Boston, Massachusetts.

Day, R., Fuller, M., Schmidt, V.A., 1977. Hysteresis properties of titanomagnetites; grain-size and compositional dependence. Physics of the Earth and Planetary Interiors 13, 260–267.

Dunne, W.M., Onasch, C.M., Williams, R.T., 1990. The problem of strain-marker centers and the Fry method. Journal of Structural Geology 12, 933–938.

Engelder, T., 1979. The nature of deformation within the outer limits of the central Appalachian fold–thrust belt in New York State. Tectonophysics 55, 289–310.

Epstein, J.B., Lyttle, P.T., 1987. Structure and stratigraphy above, below, and within the Taconic unconformity, southeastern New York (Trip C). In: Waines, R.H. (Ed.), Field Trip Guidebook, Annual Meeting of the New York State Geological Association. New York State Geological Survey, vol. 59, Albany, pp. C1–C78.

Erslev, E.A., 1988. Normalized center-to-center strain analysis of packed aggregates. Journal of Structural Geology 10, 201–209.

Evans, M.A., Elmore, R.D., 2006. Fluid control of localized mineral domains in limestone pressure solution structures. Journal of Structural Geology 28, 284–301.

Fisher, D.W., 1962. Correlation of the Ordovician Rocks of New York State. New York State Museum, Albany, New York.

Fry, N., 1979. Random point distributions and strain measurement in rocks. Tectonophysics 60, 89–105.

Fuller, M.D., 1964. On the magnetic fabrics of certain rocks. Journal of Geology 72, 368–376.

Gray, M.B., Mitra, G., 1999. Ramifications of four-dimensional progressive deformation in contractional mountain belts. Journal of Structural Geology 21, 1151–1160.

Gray, M.B., Stamatakos, J., 1997. New model for evolution of fold and thrust belt curvature based on integrated structural and paleomagnetic results from the Pennsylvania Salient. Geology (Boulder) 25, 1067–1070.

Hargraves, R.B., Johnson, D., Chan, C.Y., 1991. Distribution anisotropy; the cause of AMS in igneous rocks? Geophysical Research Letters 18, 2193–2196.

Harrison, M.J., 2002. Origin, Architecture, and Thermal State of the Lackawanna Synclinorium, Pennsylvania; Implications for Tectonic Evolution of the Central Appalachians. Ph.D. thesis, University of Illinois at Urbana-Champaign.

Harrison, M.J., 2006. Fold–thrust belt structures of the Lackawanna synclinorium, Pennsylvania: insight into the tectonic evolution of the central Appalachians. Northeastern Geology and Environmental Sciences 28, 358–367.

Harrison, M.J., Marshak, S., McBride, J.H., 2004. The Lackawanna synclinorium, Pennsylvania; a salt-collapse structure, partially modified by thin-skinned folding. Geological Society of America Bulletin 116, 1499–1514.

Harrison, M.J., Onasch, C.M., 2000. Quantitative assessment of low-temperature deformation mechanisms in a folded quartz arenite, Valley and Ridge Province, West Virginia. Tectonophysics 317, 73–91.

Hrouda, F., 1982. Magnetic anisotropy of rocks and its application in geology and geophysics. Geophysical Surveys 5, 37–82.

Jelinek, V., 1978. Statistical processing of anisotropy of magnetic susceptibility measured on groups of specimens. Studia Geophysica et Geodetica 22, 50–62.

Jelinek, V., Pokorny, J., Richter, A.K., 1997. Some new concepts in technology of transformer bridges for measuring susceptibility anisotropy of rocks. Physics and Chemistry of the Earth 22, 179–181.

Kissel, C., Barrier, E., Laj, C., Lee, T.Q., 1986. Magnetic fabric in "undeformed" marine clays from compressional zones. Tectonics 5, 769–781.

Kligfield, R., Lowrie, W., Dalziel, I.W.D., 1977. Magnetic susceptibility anisotropy as a strain indicator in the Sudbury basin, Ontario. Tectonophysics 40, 287–308.

Latta, D.K., Anastasio, D.J., 2007. Multiple scales of mechanical stratification and décollement fold kinematics, Sierra Madre Oriental foreland, northeast Mexico. Journal of Structural Geology 29, 1241–1255.

Laporte, L.F., 1969. Carbonate facies of the Helderberg Group (Lower Devonian) of New York, Trip 9. In: Guidebook for Field Trips in New York, Massachusetts, and Vermont 61. New England Intercollegiate Geological Conference, Albany, 9-1.

Lowrie, W., Hirt, A.M., 1987. Anisotropy of magnetic susceptibility in the Scaglia Rossa pelagic limestone. Earth and Planetary Science Letters 82, 349–356.

Lüeneburg, C.M., Lampert, S.A., Lebit, H.D., Hirt, A.M., Casey, M., Lowrie, W., 1999. Magnetic anisotropy, rock fabrics and finite strain in deformed sediments of SW Sardinia (Italy). Tectonophysics 307, 51–74.

Marshak, S., 1986. Structure and tectonics of the Hudson Valley fold–thrust belt, eastern New York State. Geological Society of America Bulletin 97, 354–368.

Marshak, S., 1990. Structural Geology of Silurian and Devonian Strata in the Mid-Hudson Valley, New York: Fold–Thrust Belt Tectonics in Miniature. New York State Museum, Albany, New York.

Marshak, S., 2004. Salients, recesses, arcs, orocines, and syntaxes – a review of ideas concerning the formation of map-view curves in fold–thrust belts. In: McClay, K.R. (Ed.), Thrust Tectonics and Hydrocarbon Systems, Memoir 82. AAPG, pp. 131–156.

Marshak, S., Engelder, T., 1985. Development of cleavage in limestones of a fold–thrust belt in eastern New York. Journal of Structural Geology 7, 345–359.

Marshak, S., Tabor, J.R., 1989. Structure of the Kingston Orocline in the Appalachian fold–thrust belt, New York. Geological Society of America Bulletin 101, 683–701.

Marshak, S., Wilkerson, M.S., 1992. Effect of overburden thickness on thrust-belt geometry and development. Tectonics 11, 560–566.

Onasch, C.M., 1994. Assessing brittle volume-gain and pressure solution volume-loss processes in quartz arenite. Journal of Structural Geology 16, 519–530.

Onasch, C.M., Dunne, W.M., 1993. Variation in quartz arenite deformation mechanisms between a roof sequence and duplexes. Journal of Structural Geology 15, 465–475.

Onasch, C.M., Shen, T.B., Couzens, S.B.A., 1998. Strain partitioning and factorization in a quartz arenite. Journal of Structural Geology 20, 1065–1074.

Parés, J.M., van der Pluijm, B.A., Dinares, T.J., 1999. Evolution of magnetic fabrics during incipient deformation of mudrocks (Pyrenees, northern Spain). Tectonophysics 307, 1–14.

Parés, J.M., van der Pluijm, B.A., 2002. Evaluating magnetic lineations (AMS) in deformed rocks. Tectonophysics 350, 283–298.

Parés, J.M., van der Pluijm, B.A., 2003. Magnetic fabrics and strain in pencil structures of the Knobs formation, Valley and Ridge Province, US Appalachians. Journal of Structural Geology 25, 1349–1358.

Paterson, S.R., Yu, H., 1994. Primary fabric ellipsoids in sandstones; implications for depositional processes and strain analysis. Journal of Structural Geology 16, 505–517.

Ramsay, J.G., Wood, D.S., 1973. The geometric effects of volume change during deformation processes. Tectonophysics 16, 263–277.

Rathore, J.S., 1979. Magnetic susceptibility anisotropy in the Cambrian slate belt of North Wales and correlation with strain. Tectonophysics 53, 83–97.

Rickard, L.V., 1962. Late Cayugan (Upper Silurian) and Helderbergian (Lower Devonian) Stratigraphy of New York. New York State Museum Bulletin, Albany, New York.

Rochette, P., 1987. Magnetic susceptibility of the rock matrix related to magnetic fabric studies. Journal of Structural Geology 9, 1015–1020.

Rodgers, J., 1971. The Taconic orogeny. Geological Society of America Bulletin 82, 1141–1178.

Saint-Bezar, B., Hebert, R.L., Aubourg, C., Robion, P., Swennen, R., Frizon, d.L.D., 2002. Magnetic fabric and petrographic investigation of hematite-bearing sandstones within ramp-related folds; examples from the South Atlas Front (Morocco). Journal of Structural Geology 24, 1507–1520.

Tarling, D.H., Hrouda, F., 1993. The Magnetic Anisotropy of Rocks. Chapman & Hall, London.

Treagus, S.H., 2002. Modelling the bulk viscosity of two-phase mixtures in terms of clast shape. Journal of Structural Geology 24, 57–76.

Waines, R.H., 1976. Stratigraphy and paleontology of the Binnewater Sandstone from Accord to Wilbur, New York (Trips B-3 and C-3). In: Johnsen, J.H. (Ed.), Guidebook to Field Excursions. New York State Geological Association, vol. 8, Albany, 15 pp.

Waines, R.H., 1986. The Quassaic Group, a Medial to Late Ordovician arenite sequence in the Marlboro Mountains Outlier, mid-Hudson Valley, New York, U.S.A. Geological Journal 21, 337–351.

Waines, R.H., Hoar, F.G., 1967. Upper Silurian–Lower Devonian stratigraphic sequence, western Mid-Hudson Valley region, Ulster County, New York. In: Guidebook to Field Excursions. New York State Geological Association, vol. 39 New Paltz, D1-D28.

Wanless, H.R., 1921. Final Report on the Geology of the Rosendale Cement District. Masters thesis, Princeton.

Wetmore, P.H., 2003. Investigation into the Tectonic Significance of Along Strike Variations of the Peninsular Ranges batholith, Southern and Baja California. Ph.D. thesis, University of Southern California.